

# Regio- and Stereoselective, Intramolecular [2 + 2] Cycloaddition of Allenes, Promoted by Visible Light Photocatalysis

Milos Jovanovic,<sup>a</sup> Predrag Jovanovic,<sup>a</sup> Gordana Tasic,<sup>a</sup> Milena Simic,<sup>a</sup>  
Veselin Maslak,<sup>b</sup> Srdjan Rakic,<sup>c</sup> Marko Rodic,<sup>c</sup> Filip Vlahovic,<sup>d</sup>  
Milos Petkovic,<sup>a,\*</sup> and Vladimir Savic<sup>a,\*</sup>

<sup>a</sup> University of Belgrade, Faculty of Pharmacy, Department of Organic Chemistry, Vojvode Stepe 450, 11221, Belgrade, Serbia  
E-mail: vladimir.savic@pharmacy.bg.ac.rs; milosp@pharmacy.bg.ac.rs

<sup>b</sup> University of Belgrade, Faculty of Chemistry, Department of Organic Chemistry, Studentski Trg 16, 11000, Belgrade, Serbia

<sup>c</sup> University of Novi Sad, Faculty of Sciences, Trg Dositeja Obradovića 3, 21000 Novi Sad, Serbia

<sup>d</sup> University of Belgrade, Institute of Chemistry, Technology and Metallurgy, Njegoševa 12, 11000 Belgrade, Serbia

Manuscript received: March 30, 2023; Revised manuscript received: July 4, 2023;

Version of record online: July 18, 2023



Supporting information for this article is available on the WWW under <https://doi.org/10.1002/adsc.202300301>

**Abstract:** Enallenylamides have been utilized for the synthesis of heterobicyclo[4.2.0]octane derivatives via Ir/hv promoted [2 + 2] cycloaddition reaction. The reaction specifically targets the distal double bond of the allene moiety, and results in the exclusive formation of the *trans* product. The process is conducted at room temperature and under an inert atmosphere. An extensive study on the substituent propensities during the cycloaddition step revealed variable effects. Electron-withdrawing groups conjugated with the double bond participating in the cycloaddition either hindered the process or reduced its yield. Conversely, electron-donating substituents enhanced the efficiency, resulting in product yields ranging from 60% to 88%. Our study also demonstrated the influence of protecting groups on the reaction pathway.

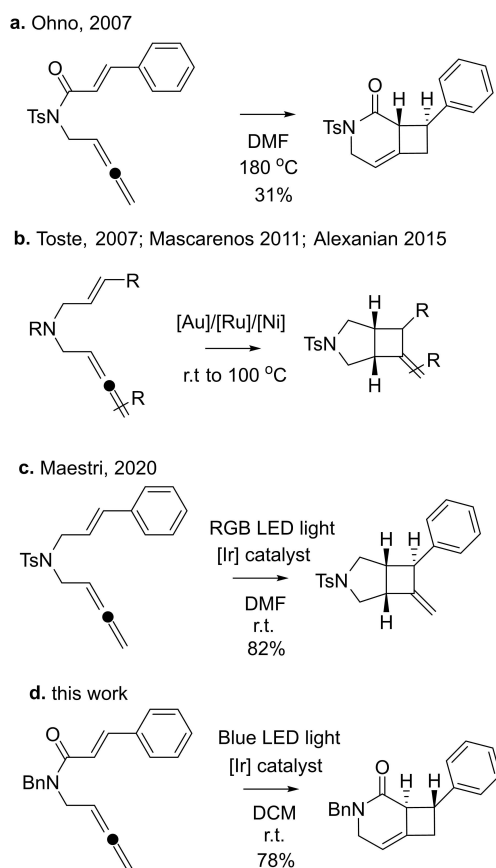
**Keywords:** [2 + 2] cycloaddition; allenes; photochemistry; photocatalysis; iridium; DFT

In recent decades, there has been extensive research on the chemical reactivity of allenes, resulting in the development of numerous efficient and reliable synthetic methodologies.<sup>[1]</sup> The unique structural properties and reactivity of these molecules make them useful partners in many processes, particularly those promoted by various metal salts.<sup>[2]</sup> Primarily, allenes have been used as 2-C synthons in the cyclisation reactions involving either of the double bonds, ranging from [2 + 1] to [6 + 2] processes.<sup>[3]</sup> Their use as 3-C synthons has received less attention, although several synthetic

methodologies have been reported in the literature, with Lu reaction being, perhaps, the best known transformation of that type.<sup>[3f,4]</sup>

Allenes have proven to be excellent 2π components in [2 + 2] cycloaddition reactions leading to the formation of cyclobutanes as well as related 4-membered heterocyclic compounds.<sup>[5]</sup> According to Woodward-Hoffmann rules, [2 + 2] cycloadditions cannot proceed in a concerted manner under thermal conditions, but they are still possible as stepwise processes via biradical intermediates. Thermal reactions of this type involving allenes require high temperatures and tend to exhibit lower levels of regio- and stereoselectivity, particularly in intermolecular transformations.<sup>[6]</sup> Intramolecular thermal [2 + 2] cycloadditions of allenes can occur on either the proximal or distal double bond of allene resulting in condensed cyclobutane derivatives. Besides thermal conditions, photochemical conditions have also been extensively used.<sup>[7]</sup> Most of the studied examples involve enones or related compounds as allene partners in the cycloaddition process. In recent years, various methodologies involving visible light in conjunction with transition metals or other sensitizers have been developed.<sup>[8]</sup> Versatile metal catalysis has also found its place in [2 + 2] cycloadditions of allenes.<sup>[9]</sup>

As a part of our general interest in the chemistry of allenes, we report our results on intramolecular [2 + 2] cycloadditions of cinnamic acid-derived allenylamides promoted by visible light in the presence of a metal catalyst. Related thermal cycloadditions of the similar substrates were reported by Ohno in 2007 (Scheme 1a).<sup>[10]</sup> The cinnamic allenylamides afforded products with *trans* stereochemistry, with yields reaching approximately 30%. However, other similar exam-



**Scheme 1.** Intramolecular [2 + 2] cycloadditions of allenenes.

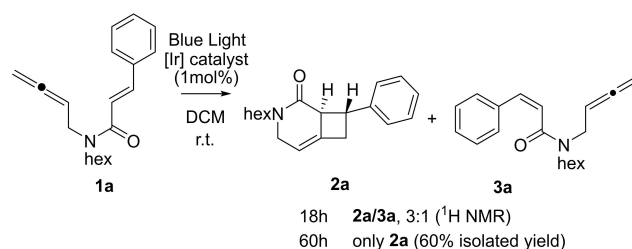
ples lacking amide functionality proved to be more efficient. The Toste group demonstrated the efficient application of Au-catalysis in the same processes.<sup>[11]</sup> The [2 + 2] cycloadducts were obtained under mild conditions in very good yields. The use of chiral dinuclear gold(I)-biarylphosphine complexes enabled highly enantioselective synthesis of cyclobutane derivatives (Scheme 1b). Furthermore, Alexanian and Mascarenas groups demonstrated the application of Ni- and Ru-complexes for similar purposes.<sup>[12]</sup> A recent report by Maestri described the photochemical conditions for performing intramolecular [2 + 2] cycloadditions of enallenes, (Scheme 1c).<sup>[13]</sup> In most cases, cyclobutane derivatives were obtained in very good yields with a high level of diastereoselectivity. In all these examples, the stereochemistry of the alkene moiety was preserved in the cycloadducts. While the thermal conditions generated products involving distal double bond of the allene functionalities, metal catalysis or metal/photochemical catalysis afforded cycloadducts corresponding to the reaction of the proximal double bond. In our reported process (Scheme 1d), we employ photochemical conditions combined with Ir-catalysis. It is worth noting the exclusive involvement of the distal double bond in the cycloaddition step and the formation of

*trans*-cyclobutane products. Thus, with these features, our method can be used as complementary to the previously reported photochemical process by Maestri. Additionally, although the thermal processes of the same substrate provide access to the cyclobutane products, they are significantly less efficient than the photochemical transformations reported herein.

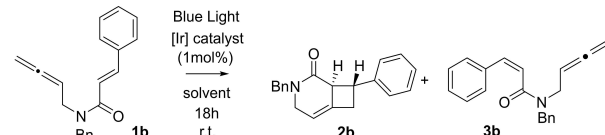
As a part of our interest in heterobicycle[4.2.0]octane structures, we explored the photochemically promoted [2 + 2] cycloaddition of enallenylamides as a relatively straightforward route to access some of these compounds. The initial experiments were outlined in Scheme 2. The reaction was performed in DCM with 1 mol% of iridium catalyst at room temperature employing exclusively *E*-cinnamic amide derivative **1a**. Inspection of <sup>1</sup>H NMR of the crude mixture after 18 h of irradiation with blue light indicated the formation of two products, cycloadduct **2a** and isomerized enallenylamide **3a** in a 3:1 ratio, respectively. Continuation of the process for an additional 42 h resulted in complete conversion and formation of **2a** only isolated in 60% yield. NMR analysis of the crude mixture showed the involvement of only distal double bond. This observation was in contrast with above-mentioned Ir/hv catalysis developed by Maestri. On the other hand, under mild conditions the reaction seemed to be more efficient than the corresponding thermal process.

Following these initial results, we screened various conditions to optimize the transformation, (Table 1). All reactions were performed at room temperature with 1 mol% of the catalyst and irradiated with blue led light.

Among the several catalysts, Ir(ppy)<sub>3</sub> (Table 1, entries 5 and 10) proved to be the most efficient, either in MeCN or DCM as a solvent affording only cycloadduct **2b** in 74% or 78% isolated yield respectively. Comparable efficiency in both solvents was demonstrated by [Ir{dF(CF<sub>3</sub>)ppy}<sub>2</sub>(dtbpy)]PF<sub>6</sub> (Table 1, entries 3 and 8) while [Ir(dtbbpy)(ppy)<sub>2</sub>][PF<sub>6</sub>] (Table 1, entries 4 and 9), interestingly, showed solvent dependent properties. In MeCN, it afforded 68% of **2b** (accompanied by 27% of isomerized **3b**) whereas in DCM, it afforded 17% of **2b** (accompanied by 78% of isomerized **3b**). These processes are likely initiated by



**Scheme 2.** Cycloaddition of enallene **1a**.

**Table 1.** Reaction optimization with substrate **1b**.


Entry	Catalyst	Solvent	NMR Yield <sup>[b]</sup> (%)			Yield, <sup>[c]</sup> <b>2b</b> (%)
			<b>1b</b>	<b>2b</b>	<b>3b</b>	
1	Ru(bpy) <sub>3</sub> (PF <sub>6</sub> ) <sub>2</sub>	MeCN	66	3	31	
2	[Ru(phen) <sub>3</sub> ]Cl <sub>2</sub>	MeCN	97	3	/	
3	[Ir{dF(CF <sub>3</sub> )ppy} <sub>2</sub> (dtbpy)]PF <sub>6</sub>	MeCN	/	81	/	
4	[Ir(dtbbpy)(ppy) <sub>2</sub> ][PF <sub>6</sub> ]	MeCN	/	68	27	
5	Ir(ppy) <sub>3</sub>	MeCN	/	85	/	74
6	Ru(bpy) <sub>3</sub> (PF <sub>6</sub> ) <sub>2</sub>	DCM	90	4	5	
7	[Ru(phen) <sub>3</sub> ]Cl <sub>2</sub>	DCM	96	4	/	
8	[Ir{dF(CF <sub>3</sub> )ppy} <sub>2</sub> (dtbpy)]PF <sub>6</sub>	DCM	/	81	/	
9	[Ir(dtbbpy)(ppy) <sub>2</sub> ][PF <sub>6</sub> ]	DCM	/	17	78	
10	Ir(ppy) <sub>3</sub>	DCM	/	89	/	78
11	No catalyst	DCM	100	/	/	
12	Ir(ppy) <sub>3</sub> , No light	DCM	100	/	/	

<sup>[a]</sup> Reaction conditions: **1b** 0.06 mmol, Ir-catalyst 1 mol%, solvent 3 mL, blue led light strip, r.t.;

<sup>[b]</sup> Yields of **1b/2b/3b** established by <sup>1</sup>H NMR, using pyridine as a standard;

<sup>[c]</sup> Isolated yields.

energy transfer from the photocatalyst in its triplet state to alkene double bond leading to the excited alkene triplet state and followed by further cyclisation.<sup>[14]</sup> For the process to be feasible, it is necessary for the triplet energy states of both reaction components to be in a similar range, while the triplet excited-state energy of the photocatalyst needs to be higher than that of both components. Performing the reaction outlined in Table 1 with Ru(bpy)<sub>3</sub>(PF<sub>6</sub>)<sub>2</sub>, triplet energy ( $E_T$ ) 46 kcal/mol, yielded only 3% of cycloadduct **2b** and 31% of isomerized product **3b** in MeCN.<sup>[15]</sup> This suggests that  $E_T$  for the catalyst is lower than that for the alkene moiety of cinamic amides (e.g. calculated  $E_T$ -**1c** 48.1 kcal/mol). The observed results also indicate that the isomerization to form *Z*-alkene is somewhat faster than the cycloaddition, while the formation of triplet state *Z*-alkene, leading either to *Z/E* isomerization or cycloaddition, is not possible due to the higher  $E_T$  of the *Z* isomer. On the other hand, employing [Ir(dtbbpy)(ppy)<sub>2</sub>][PF<sub>6</sub>],  $E_T$  51 kcal/mol, resulted in a slightly better outcome in MeCN, yielding **2b** and **3b** in 2.5:1 ratio. Interestingly the result was the opposite in DCM as a solvent.

Finally, further increase in catalyst  $E_T$ , ([Ir{dF(CF<sub>3</sub>)ppy}<sub>2</sub>(dtbpy)]PF<sub>6</sub>,  $E_T$  62 kcal/mol; Ir(ppy)<sub>3</sub>,  $E_T$  55 kcal/mol) resulted in much better outcomes producing only cycloadduct **2b** in both cases. Two additional experiments, one without a catalyst and another without blue LED light, demonstrated detrimental role of both reaction components (Table 1, entries 11, 12). After establishing the optimal reaction conditions, the

scope of the transformation was further explored. The preliminary optimization results (Table 1) showed that both MeCN and DCM were equally effective as solvents, with an indication that it will not be always the case. Specifically, [Ir(dtbbpy)(ppy)<sub>2</sub>][PF<sub>6</sub>] exhibited notable differences in performance between the two solvents. Therefore, we decided to investigate the scope of this process in both MeCN and DCM, as summarized in Table 2. While variations of *N*-protecting group were expected to have minimal impact on the reaction, the results indicated otherwise. For instance, acetyl protection (Table 2, entry 3) did not have any negative influence on the reaction, resulting in full conversion after 18 h and 72% yield of cycloadduct **2c**. Performing the same transformation with the *N*-phenyl derivative (Table 2, entry 5) gave different results. After 18 hours, the reaction in MeCN resulted in a 12:88 ratio of the starting compound **1e** to the isomerized product **3e**, with no observable cycloadduct **2e**. Conversely, conducting the same reaction in DCM led to a 5:95 ratio of isomerized product **3e** to cycloadduct **2e**. Moreover, by extending the reaction time it was possible to exclusively obtain the desired product in 72% yield. The most remarkable effect was demonstrated with the *N*-Boc protecting group (Table 2 entry 4). Under the same conditions in both MeCN and DCM, the reaction predominantly produced the isomerized product **3d** (contributing to 81–93% of the reaction mixture), while cycloadduct **2d** was not formed in significant amounts. These results can be attributed to the conformational prefer-

**Table 2.** Scope of the reaction.

Variation of N-protecting group	Entry <sup>[a]</sup>	Compound	MeCN			DCM			2 <sup>[c]</sup> (%)			
			18h <sup>[b]</sup>			60h <sup>[b]</sup>						
			1	2	3	1	2	3		1	2	3
 1a-e	1	1a, R <sup>3</sup> = <i>n</i> -hex	67	33	93	7	76	24	100	<b>60</b>		
	2	1b, R <sup>3</sup> = Bn	100				100			<b>78</b>		
	3	1c, R <sup>3</sup> = Ac	100				100			<b>72</b>		
	4	1d, R <sup>3</sup> = Boc	14	86	19	81	7	93	19	81	/	
	5	1e, R <sup>3</sup> = Ph	12	88			95	5	100 <sup>[d]</sup>		<b>72</b>	
Variation of aromatic component												
 1f-n, 1p-s	6	1f, R = 4-OH	100				100			<b>80</b>		
	7	1g, R = 2-OMe	96	4			95	5		<b>86</b>		
	8	1h, R = 3-OMe	73	27			100			<b>88</b>		
	9	1i, R = 4-OMe	100				100 <sup>[e]</sup>			<b>88</b>		
	10	1j, R = 2,6-OMe		100		100	22	78			/	
 1k-o	11	1k, R = 4-Cl	69	31	100		97	3		<b>50</b>		
	12	1l, R = 2-Cl	24	76			49	51	61	39	<b>39</b>	
	13	1m, R = 2-NO <sub>2</sub>	62	6	32	5	95				/	
	14	1n, R = 3-NO <sub>2</sub>	100				55	6	39	14	19	67
	15	1o, R = 3-NO <sub>2</sub>					59	41			/	
 1p-u	16	1p, R = 2-CF <sub>3</sub>	23	77	26	74	8	23	69	26	74	/
	17	1q, R = 2-Me	29	71	97	3	100					<b>80</b>
	18	1r, R = 3-Me	64	36	94	6	96	4		100 <sup>d</sup>		<b>62</b>
	19	1s, R = 4-Me	27	73	100		84	16		100		<b>60</b>
	20	1t, R <sup>4</sup> = 2-pyridinyl	20	80	36	64	100					<b>41</b>
	21	1u, R <sup>4</sup> = 2-furanyl	100				100					<b>76</b>
Other variations												
 1v-x	22	1v	100				100				<b>82</b>	
	23	1w	100				100				<b>89</b>	
	24	1x	100								/	

<sup>[a]</sup> Reaction conditions: **4** 0.06 mmol, Ir-catalyst 1 mol%, solvent 3 mL, blue led light strip (10 m, 12 V DC, 4.8 W), r.t.;

<sup>[b]</sup> Ratios of **1/2/3** established by <sup>1</sup>H NMR;

<sup>[c]</sup> Isolated yields for reactions performed in DCM after sufficient time;

<sup>[d]</sup> 36 h;

<sup>[e]</sup> After 45 minutes the reaction mixture contained 33% of *Z* isomer and 67% of cycloadduct **1i**.

ences of the tertiary amide with N–Boc protection. For the cycloaddition to take place, two double bonds that participate in the reaction should be positioned in close

proximity. However, our DFT calculations (see SI) indicate that these conformations are unfavorable, rendering the Boc derivative unreactive in this process.

We further studied various substituted cinnamic amides utilizing N-benzyl protecting group. Compound **1f**, possessing *p*-OH substituent, reacted efficiently, affording cycloadduct after 18 h with full conversion and isolated yield of 80%. Similarly, compound **1i** (Table 2, entry 9) with an OMe substituent in place of the OH, yielded a comparable outcome. Interestingly, upon inspecting the reaction mixture after 45 minutes, it was observed that the cycloadduct **2i** was formed in 67% yield, while the remaining 33% consisted of the *Z* isomer. This suggests that both the *E* and *Z* isomers readily undergo conversion to the cycloadduct **2i** in this particular case. Further examples demonstrated that the position of MeO influences the product yield. Thus, the *o*-MeO derivative **1g** (Table 2, entry 7) and, in particular, *m*-MeO derivative **1h** (Table 2, entry 8) gave a mixture of isomerized product and cycloadduct, with a preference for the latter (4:96 and 27:73, respectively). The choice of solvent did not significantly impact the reaction outcome for **1g**. However, for the *m*-MeO derivative **1h**, changing the solvent from MeCN to DCM resulted in the formation of the pure cycloadduct in 88% yield after 18 hours. Introducing the second MeO group (Table 2, entry 10) hindered the reaction as the 2,6-dimethoxy derivative **1j** predominantly produced the isomerized product in MeCN even with prolonged reaction time, while in DCM, only 22% of the cycloadduct was formed after 18 hours. Overall, electron donating groups promote the cycloaddition, with *m*-MeO being slightly less effective, but its efficiency can be improved by choosing the appropriate solvent. The presence of the weaker electron-donating Me-group at all three positions of the aromatic ring, compounds **1q–s** (Table 2, entries 17–19), led to variable results. However, by modifying the reaction conditions, it was possible to shift the reaction towards the exclusive formation of the cycloadducts in all three cases, with yields ranging from 60% to 80%.

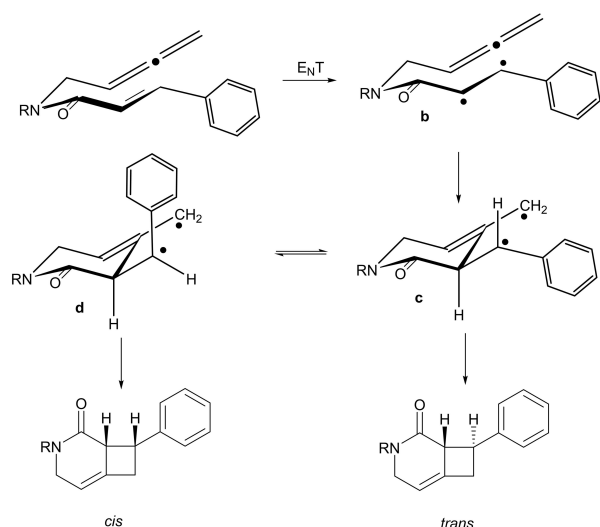
Substrates with electron-withdrawing properties were also examined. The, NO<sub>2</sub>-derived compounds, **1m–o**, proved to be very resistant to the cycloaddition process. Under various conditions (Table 2, entries 13–15), the starting compound was the dominant component in the reaction mixture, indicating an inhibitory effect of the strong electron-withdrawing group on the cycloaddition step. This was further confirmed with the another strong electron-withdrawing group (CF<sub>3</sub>) (Table 2, entry 16), which predominantly yielded the isomerized product. Weaker electron-withdrawing substituents, such as chlorine, showed a similar trend, although less pronounced than the NO<sub>2</sub> group. The *p*-Cl derivative **1k**, when subjected to various conditions in MeCN for 60 hours, yielded only the cycloadduct, while in DCM, a similar result was obtained with traces of isomerized product observed. However, the isolated yield of **2k** was only 50% (Table 2,

entry 11). When *o*-Cl isomer **1l** was used, all experiments resulted in a mixture of isomerized product and the desired cycloadduct, which was isolated in 39% yield. These results clearly indicate that electron-donating substituents on the aromatic ring of cinnamic amides bearing proximal allenic functionality are better promoters of the [2+2] cycloaddition reactions under the described conditions than their electron-withdrawing counterparts.

Further exploration of the reaction scope involved the replacement of the benzene ring in cinnamic amides with heterocyclic rings which confirmed the above observations to some extent (Table 2 entries 20, 21). The introduction of a pyridine ring (Table 2, entry 20) slowed down the cycloaddition reactions in MeCN but in DCM the only observed product after 18 h was the cycloadduct, isolated in a modest yield of 41%. In contrast, the furan derivative **1u** (Table 2, entry 21) in MeCN exclusively gave cycloaddition product after 18 h with a higher yield of 76%. Replacing benzene ring with the conjugated double bond, as seen in **1v** (Table 2, entry 22), did not affect the reactivity as the cycloadduct was the only observed product, isolated in 82% yield. Additionally, a single example of cycloaddition reaction with substituted allene **1w** (Table 2, entry 23) was performed. Despite the creation of a quaternary carbon atom in the cycloaddition step, the reaction was completed in 18 h in both MeCN and DCM, resulting in a high yield of the cycloadduct (89%). The high yield could be attributed to the formation of a more stable tertiary allylic radical intermediate, in contrast to the typical primary allylic intermediate observed with other substrates. Finally, the substrate **1x** (Table 2, entry 24), which lacked the extended conjugation present in other substrates, showed no reactivity under the standard conditions, with complete recovery of the starting material in MeCN after 18 hours. This highlighted the importance of additional conjugation in the reactivity of the double bond in the studied systems.

It is likely that the energy transfer process outlined in Scheme 3 is operational in the above transformations. Namely, experimentally determined single electron reduction of **1a** ( $E = -2.1$  V vs Ag/AgCl or  $-2.055$  V vs SCE; Ir<sup>3+</sup>\*/Ir<sup>4+</sup>  $E = -1.7$  V vs SCE) ruled out the redox pathway. The energy transfer route was also supported by theoretical comparison of the two possible mechanisms.

The reaction is initiated by the formation of triplet state biradical **b** via an energy transfer process.<sup>[14]</sup> Subsequent cyclisation at the central allene carbon atom leads to the formation of allylic radical **c** which further undergoes cyclization to yield the final cyclobutane product. Among the two possible products *trans* and *cis*, generated from diradicals **c** and **d** (Scheme 3), the *trans* isomer would be expected to be the major product due to the pseudoequatorial orientation of the



**Scheme 3.** Stereochemistry of the cycloaddition process.

phenyl substituent.

The interpretation of ROESY experiments of **2c**, intended to assign stereochemistry, was not unambiguous and suggested the formation of the *cis* product, most likely due to the relatively close proximity of two protons (3.06 Å) in the cyclobutane ring.<sup>[16]</sup> However, crystallographic analysis of **2c** confirmed the formation of the *trans* product, as shown in Figure 1.<sup>[17]</sup> This observation supports the proposed mechanism involving biradical **b** and the generation of the allylic radical **c**, leading to the *trans* cyclobutane product. The alternative mechanism involving the terminal carbon atom of the allenic functionality is less likely, as it would require the formation of a less favored eight-membered ring and a less stable vinyl radical in place of an allyl radical.

We further studied the above process by computational modelling of all terminal molecular species, intermediates and transition states along the reaction pathway by means of Density Functional Theory (DFT).<sup>[18]</sup> This study was particularly focused on differences in reactivity of representative molecules **1o** and **1y**<sup>[19]</sup> possessing electron-withdrawing or electron-

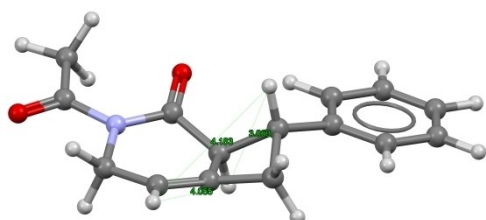


**Figure 1.** Molecular structure of **2c** with numeration of relevant atoms. Selected distances:  $d(\text{H1}\cdots\text{H8})=3.063$  Å;  $d(\text{H1}\cdots\text{H5})=4.055$  Å;  $d(\text{H5}\cdots\text{H8})=4.183$  Å.

donating aryl substituents in comparison with the parent **1c**. Calculated triplet state energy ( $E_T$ ) of the employed catalyst,  $E_T=54.3$  kcal/mol, is sufficient to promote excitation of all three reactants ( $E_T$  **1c**, **1o**, **1y**=48.1–48.9 kcal/mol) via the energy transfer mechanism (Figure 2). In optimized triplet states  $t_1$  of **1c** ( $t_1$ ) and **1o** ( $t_1$ ), C-atoms of the excited alkene moiety are perpendicular to each other. From this state both structures can return to the ground state by C–C bond rotation yielding either *E*- or *Z*-isomer or can adopt TS1 to produce cycloadducts.<sup>[14,20]</sup> Derivative **1y** ( $t_2$ ) in the excited state  $t_2$  retained its initial ground-state geometry although an equienergetic triplet state, corresponding to the  $t_1$  geometry, exists. We believe that in this state, with the planar geometry, **1y** ( $t_2$ ) prefers the thermodynamically more favorable path via TS1, affording the cycloadduct **2y**. Our experimental results demonstrated that the isomerisation occurred in the reactions with all three compounds. Obviously, the products of photoisomerization, *Z*-alkene, can undergo another excitation to the triplet state and return to the *E*-alkene ground state via the  $t_1$  excited state or divert to the cycloaddition product. Calculated values of  $E_T$  for *Z* substrate **1o'** indicate the triplet state energy of the photocatalyst is now insufficient to establish sensitization in this case. Furthermore, as illustrated in Figure 1, the spin density of the **1o** ( $t_3$ ) triplet state  $t_3$  has shifted from the double bond to the aromatic ring, likely due to the electron-withdrawing effect of the group, which decreases the probability for an effective bond rotation promoting pathway via TS1. These results demonstrated the detrimental effect of the aryl substituent on the studied reaction pathway emphasizing the need for careful planning of the reacting partners.<sup>[22]</sup>

In conclusion, we developed intramolecular [2+2] cycloadditions of cinnamic acid-derived allenic amides, providing a complementary route to existing methodologies for the synthesis of heterobicyclo[4.2.0]. Described methodology provides access to *trans*-product exclusively in good yields. A high degree of regioselectivity, i.e. reaction with the distal double bond of the allene moiety, corresponds to the results observed in the thermal processes, but it is opposite to the related photochemical transformations which favored involvement of the proximal double bond. Furthermore, our studies have highlighted the significant influence of the substituents attached to the aromatic ring on the reaction outcome. Careful consideration of these substituents is crucial when planning synthetic strategies involving this methodology. Finally, the process does not seem to be hindered by the formation of the sterically more demanding quaternary C-atom at the cyclobutane ring.

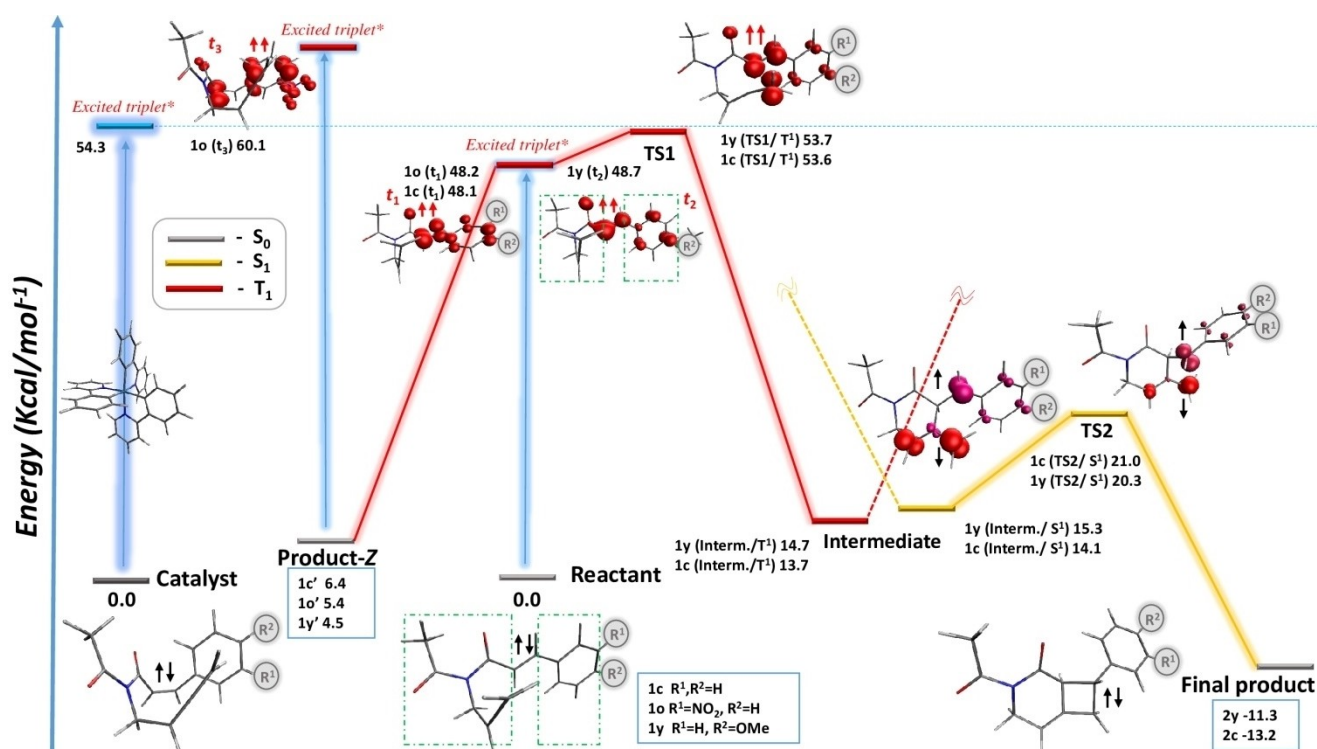


Figure 2. Schematic representation of the photocatalyzed reaction of compounds **1c**, **1o** and **1y**.<sup>[21]</sup>

## Experimental section

To a dram vial equipped with magnetic stir bar were added alleneamide (0.06 mmol), Ir(ppy)<sub>3</sub> (1 mol%) and DCM (3 mL). The solution was sparged with nitrogen, sealed and irradiated with Blue LED strips (distance from the light source 12 cm) for 18–60 hours at room temperature. Conversion was monitored by TLC. Upon completion the reaction mixture was concentrated under reduced pressure and purified by flash chromatography on silica gel (mesh 230–400) using petroleum ether and diethyl ether.

## Acknowledgements

This research was funded by the Ministry of Education, Science and Technological Development, Republic of Serbia through Grant Agreement with University of Belgrade-Faculty of Pharmacy No: 451-03-68/2022-14/200161. We thank Dr Dusan Ruzic, University of Belgrade, Faculty of Pharmacy, for performing initial computational calculations and Dr Aleksandra Mitrovic, University of Belgrade, Faculty of Chemistry for performing CV experiment. We are also thankful to Dr Radomir Saicic, University of Belgrade, Faculty of Chemistry for fruitful discussion.

## References

- [1] a) H. Hopf, M. S. Sherburn, *Synthesis* **2022**, *54*, 864–886; b) G.-Q. Gao, G. Ma, X.-L. Jiang, Q. Liu, C.-L. Fan, D.-C. Lv, H. Su, G.-X. Ru, W.-B. Shen, *Org.*

*Biomol. Chem.* **2022**, *20*, 5035–5044; c) S. K. Nanda, R. Mallik, *Asian J. Org. Chem.* **2022**, *11*, 41–65; d) J. Singh, A. Sharma, A. Sharma, *Org. Chem. Front.* **2021**, *8*, 5651–5667; e) J. M. Alonso, P. Almendros, *Chem. Rev.* **2021**, *121*, 4193–4252; f) M. D. Jovanovic, M. R. Petkovic, V. M. Savic, *Synthesis* **2021**, *53*, 1035–1045; g) R. Blicek, M. Taillefer, F. Monnier, *Chem. Rev.* **2020**, *120*, 13545–13598; h) L. Liu, R. M. Ward, J. M. Schomaker, *Chem. Rev.* **2019**, *119*, 12422–12490; i) S. Arai, *Chem. Pharm. Bull.* **2019**, *67*, 397–403; j) C. Aubert, L. Fensterbank, P. Garcia, M. Malacria, A. Simonneau, *Chem. Rev.* **2011**, *111*, 1954–1993.

- [2] a) X.-L. Han, P.-P. Lin, Q. Li, *Chin. Chem. Lett.* **2019**, *30*, 1495–1502; b) A. Lledo, A. Pla-Quintana, A. Roglans, *Chem. Soc. Rev.* **2016**, *45*, 2010–2023; c) M. Munoz, *Org. Biomol. Chem.* **2012**, *10*, 3584–94; d) M. Jeganmohan, C.-H. Cheng, *Chem. Commun.* **2008**, 3101–3117; e) S. Ma, *Acc. Chem. Res.* **2003**, *36*, 701–712.
- [3] a) X. Zhong, J. Tan, J. Qiao, Y. Zhou, C. Lv, Z. Su, S. Dong, X. Feng, *Chem. Sci.* **2021**, *12*, 9991–9997; b) J. Yang, Q. Sun, N. Yoshikai, *ACS Catal.* **2019**, *9*, 1973–1978; c) J. L. Mascareñas, I. Varela, F. López, *Acc. Chem. Res.* **2019**, *52*, 465–479; d) A. Lledó, A. Pla-Quintana, A. Roglans, *Chem. Soc. Rev.* **2016**, *45*, 2010–2023; e) C. S. Adams, C. D. Weatherly, E. G. Burke, J. M. Schomaker, *Chem. Soc. Rev.* **2014**, *43*, 3136–3163; f) F. Lopez, J. L. Mascareñas, *Chem. Soc. Rev.* **2014**, *43*, 2904–2915; g) H. Clavier, K. L. Jeune, I. de Raggi, A. Tenaglia, G. Buono, *Org. Lett.* **2011**, *13*, 308–311; h) P. Mauleón, R. M. Zeldin, A. Z. González, F. D. Toste, *J.*

- Am. Chem. Soc.* **2009**, *131*, 6348–6349; i) M. R. Luzung, P. Mauleón, F. D. Toste, *J. Am. Chem. Soc.* **2007**, *129*, 12402–12403; j) M. Murakami, T. Matsuda, in *Modern Allene Chemistry*, John Wiley & Sons, Ltd, **2004**, pp. 727–815.
- [4] a) Y. Wei, M. Shi, *Org. Chem. Front.* **2017**, *4*, 1876–1890; b) X. Han, Y. Wang, F. Zhong, Y. Lu, *J. Am. Chem. Soc.* **2011**, *133*, 1726–1729.
- [5] B. Alcaide, P. Almendros, C. Aragoncillo, *Chem. Soc. Rev.* **2010**, *39*, 783–816.
- [6] a) K. Chen, R. Sun, Q. Xu, Y. Wei, M. Shi, *Org. Biomol. Chem.* **2013**, *11*, 3949–3953; b) M. R. Siebert, J. M. Osbourn, K. M. Brummond, D. J. Tantillo, *J. Am. Chem. Soc.* **2010**, *132*, 11952–11966; c) T. V. Ovaska, R. E. Kyne, *Tetrahedron Lett.* **2008**, *49*, 376–378; d) B. Alcaide, P. Almendros, C. Aragoncillo, M. C. Redondo, M. R. Torres, *Chem. Eur. J.* **2006**, *12*, 1539–1546; e) K. M. Brummond, D. Chen, *Org. Lett.* **2005**, *7*, 3473–3475; f) X. Jiang, S. Ma, *Tetrahedron* **2007**, *63*, 7589–7595.
- [7] a) B. T. Buu Hue, J. Dijkink, S. Kuiper, S. van Schaik, J. H. van Maarseveen, H. Hiemstra, *Eur. J. Org. Chem.* **2006**, 127–137; b) J. D. Winkler, J. R. Ragains, *Org. Lett.* **2006**, *8*, 4031–4033; c) E. M. Carreira, C. A. Hastings, M. S. Shepard, L. A. Yerkey, D. B. Millward, *J. Am. Chem. Soc.* **1994**, *116*, 6622–6630; d) D. Becker, M. Nagler, Y. Sahali, N. Haddad, *J. Org. Chem.* **1991**, *56*, 4537–4543.
- [8] a) X. Li, C. Jandl, T. Bach, *Org. Lett.* **2020**, *22*, 3618–3622; b) N. Arai, T. Ohkuma, *Org. Lett.* **2019**, *21*, 1506–1510; c) A. B. Rolka, B. Koenig, *Org. Lett.* **2020**, *22*, 5035–5040; d) S.-S. Zhu, J.-N. Zhou, Q.-L. Wu, W.-J. Hao, S.-J. Tu, B. Jiang, *Org. Chem. Front.* **2020**, *7*, 2975–2980.
- [9] a) W. Ding, N. Yoshikai, *Angew. Chem. Int. Ed.* **2019**, *58*, 2500–2504; b) S. Arai, Y. Kawata, Y. Amako, A. Nishida, *Tetrahedron Lett.* **2019**, *60*, 151168; c) Y. Kawata, S. Arai, M. Nakajima, A. Nishida, *Tetrahedron Lett.* **2021**, *69*, 152974; d) W.-F. Zheng, P. P. Bora, G.-J. Sun, Q. Kang, *Org. Lett.* **2016**, *18*, 3694–3697; e) M. Jia, M. Monari, Q.-Q. Yang, M. Bandini, *Chem. Commun.* **2015**, *51*, 2320–2323.
- [10] H. Ohno, T. Mizutani, Y. Kadoh, A. Aso, K. Miyamura, N. Fujii, T. Tanaka, *J. Org. Chem.* **2007**, *72*, 4378–4389.
- [11] M. R. Luzung, P. Mauleón, F. D. Toste, *J. Am. Chem. Soc.* **2007**, *129*, 12402–12403.
- [12] a) N. N. Noucti, E. J. Alexanian, *Angew. Chem. Int. Ed.* **2015**, *54*, 5447–5450; b) M. Gulías, A. Collado, B. Trillo, F. López, E. Oñate, M. A. Esteruelas, J. L. Mascareñas, *J. Am. Chem. Soc.* **2011**, *133*, 7660–7663.
- [13] A. Serafino, D. Balestri, L. Marchiò, M. Malacria, E. Derat, G. Maestri, *Org. Lett.* **2020**, *22*, 6354–6359.
- [14] F. Strieth-Kalthoff, M. J. James, M. Teders, L. Pitzer, F. Glorius, *Chem. Soc. Rev.* **2018**, *47*, 7190–7202.
- [15] a) J. Corpas, P. Mauleón, R. Gómez Arrayás, J. C. Carretero, *Adv. Synth. Catal.* **2022**, *364*, 1348–1370; b) K. Zhan, Y. Li, *Catalysts* **2017**, *7*, 337; c) J. Xu, N. Liu, H. Lv, C. He, Z. Liu, X. Shen, F. Cheng, B. Fan, *Green Chem.* **2020**, *22*, 2739–2743.
- [16] C. Redfield, in *Encyclopedia of Spectroscopy and Spectrometry* ed. J. C. Lindon, G. E. Tranter, D. W. Koppenaal, Academic Press, third edition, 2017, p. 759.
- [17] For X-ray crystallography, see: a) G. M. Sheldrick, *Acta Crystallogr. Sect. A* **2015**, *71*, 3–8; b) G. M. Sheldrick, *Acta Crystallogr. Sect. C* **2015**, *71*, 3–8; c) CCDC 2233308 contain the supplementary crystallographic data for compound **8a**. The data can be obtained free of charge from The Cambridge Crystallographic Data Centre via <https://www.ccdc.cam.ac.uk/structures/>.
- [18] W. Koch, M. C. Holthausen in *A Chemist's Guide to Density Functional Theory* Wiley-VCH: Weinheim. **2000**. xiv + 294 pp. ISBN 3–527–29918–1 2001.
- [19] To simplify DFT calculations a model compound **1y** was chosen as a representative for an electron-donating substituent due to its close resemblance to compound **1i**.
- [20] C. M. Pearson, T. N. Snaddon, *ACS Cent. Sci.* **2017**, *3*, 922–924.
- [21] The numeric values are given as the difference in Gibbs free energy relative to the energy of the ground (singlet) state of the specific compound **1c**, **1o** or **1y**.
- [22] Computational details, calculated values of HOMO–LUMO gaps as well as further discussion on main reaction pathway can be found in Supporting Information.